Article

A Model for Double Asymmetric Induction in the Stereocontrolled Reduction of Glycosyl β-Ketoesters with Oxazaborolidines

W. Harb, M. F. Ruiz-Lpez, F. Coutrot, C. Grison, and P. Coutrot

J. Am. Chem. Soc., **2004**, 126 (22), 6996-7008• DOI: 10.1021/ja031778y • Publication Date (Web): 14 May 2004

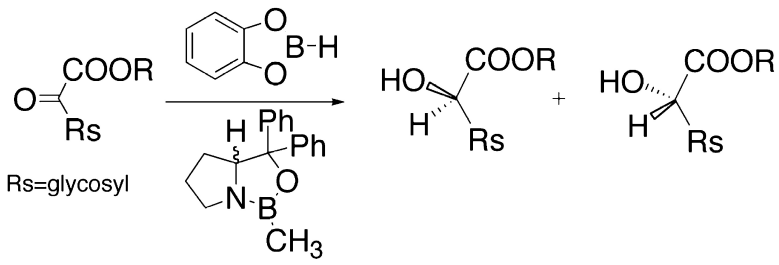

More About This Article

Additional resources and features associated with this article are available within the HTML version:

- Supporting Information
- Access to high resolution figures
- Links to articles and content related to this article
- Copyright permission to reproduce figures and/or text from this article

View the Full Text HTML

J|A|C|S
ARTICLES
Published on Web 05/14/2004

A Model for Double Asymmetric Induction in the Stereocontrolled Reduction of Glycosyl α-Ketoesters with Oxazaborolidines

W. Harb, M. F. Ruiz-López,* F. Coutrot,† C. Grison,† and P. Coutrot

Contribution from the Unité Mixte de Recherche CNRS-UHP No. 7565,‡ Université Henri Poincaré, Nancy I. BP 239, 54506 Vandoeuvre-lès-Nancy, France

Received December 17, 2003; E-mail: Manuel.Ruiz@lctn.uhp-nancy.fr

Abstract: Experimental diastereoselectivities for the stereocontrolled reduction of glycosyl α-ketoesters into the corresponding α-hydroxyesters have recently been reported with unexpected results. The process is catalyzed by a chiral oxazaborolidine derivative (the so-called CBS catalyst) and represents the key step in the synthesis of glycosyl α-amino acids synthons, a class of compounds that allow preparation of natural glycopeptides analogues exhibiting potential therapeutic relevance. Good to very good diastereomeric excesses have been obtained for a series of reactions with different glucidic derivatives, but surprisingly, the major product obtained does not correspond to that predicted by using Corey's model. In the present work, we carry out a theoretical investigation of these reactions at the density functional level. Separated effects from the catalyst and from the glucidic derivative have been computed to rationalize the observed diastereoselectivities and the double asymmetric induction.

1. Introduction

Glycoproteins are involved in many biochemical processes. In particular they play a fundamental role in a variety of molecular recognition phenomena.[1−3] A better knowledge of the properties of their elementary constituents, glycosyl amino acids and glycopeptides, would represent an important step toward the understanding of glycoprotein behavior in vivo. Accordingly, many works have been devoted to the synthesis of glycopeptides, most of them having focused on N-, O- and S-glycosyl derivatives,[4−8] inspired by the structure of natural proteins. However, these glycopeptide derivatives display a high sensitivity toward acids and bases, and therefore their synthesis is not straightforward.[9] Besides, they are subject to deglycosylation in vivo limiting their potential use as therapeutic agents.[10] Some work has also been devoted to the synthesis of the more stable C-glycosyl analogues of natural fragments where the peptide is bonded to the carbohydrate moiety by a C−C bond in anomeric position.[11−22]

Glycopeptides exhibiting a C−C bond in a nonanomeric position have received much less attention although their study appears to be a quite interesting research field. As a preliminary step in the synthesis of such a type of peptides, the corresponding glycosylated amino acid synthons with enantiomeric purity must be obtained. One possible route involves the nucleophilic amination of carboxylic acids with a leaving group in the α-position, the key step of the method being the stereocontrolled reduction of α-ketoesters into α-hydroxyesters.[23−25]

Experimental data obtained in our group[23−26] for a variety of systems have been quite encouraging. In particular, good to

† Present address: Laboratoire de Chimie Biomoléculaire, UMR 5032, Université Montpellier II, ENSCM, 8 Rue de l'Ecole Normale, 34296 Montpellier, France.

‡ Part of the Institut Nancéen de Chimie Moléculaire (INCM).

(1) Montreuil, J. *Comprehensive Biochemistry*; Neuberger, A., van Deenen, L. L., Eds.; Elsevier: Amesterdam, 1982; Vol. 19, p 1.
(2) Rodriguez, I. R.; Wheland, W. J. *J. Biochem. Biophys.* **1985**, *132*, 829.
(3) Montreuil, J.; Bouquelet, S.; Debray, H.; Fournet, B.; Spik, G.; Strecker, G. In *Carbohydrate Analysis: A Practical Approach*; Chaplin, M. F., Kennedy, J. F., Eds.; IRL: Oxford, 1986; p 143.
(4) Kessler, H.; Kottenhahn, M.; Kling, A.; Kalor, C. *Angew. Chem., Int. Ed. Engl.* **1987**, *26*, 888.
(5) Paulsen, H. *Angew. Chem., Int. Ed. Engl.* **1990**, *29*, 823.
(6) Garg, H. G.; Von Dem Bruch, K.; Kunz, H. *Adv. Carbohydr. Chem. Biochem.* **1994**, *33*, 50.
(7) Arsequell, G.; Valencia, G. *Tetrahedron: Asymmetry* **1997**, *8*, 2839.
(8) Kihlberg, J.; Elofsson, M. *Curr. Med. Chem.* **1997**, *4*, 85.
(9) Frey, O.; Hoffman, M.; Kessler, H. *Angew. Chem., Int. Ed. Engl.* **1995**, *34*, 2026 and references therein.
(10) Gottschalk, A. *Glycoproteins: Their Composition, Structure and Function*; Elsevier: New York, 1972; p 361.
(11) Hall, R. H.; Bischofberger, K.; Eitelman, S. J.; Jordaan, A. *J. Chem. Soc., Chem. Commun.* **1977**, *743*, 753.
(12) Jouillé, M. M.; Wang, P. C.; Semple, J. E. *J. Am. Chem. Soc.* **1980**, *102*, 887.
(13) Colombo, L.; Casiraghi, G.; Pittalis, A. *J. Org. Chem.* **1991**, *56*, 3897.
(14) Lieberknecht, A.; Schmidt, J.; Stezowski, J. J. *Tetrahedron Lett.* **1991**, *32*, 2113.
(15) Bertozzi, C. R.; Hoeprich, P. D., Jr.; Bednarski, M. D. *J. Org. Chem.* **1992**, *57*, 6092.
(16) Bertozzi, C. R.; Cook, D. G.; Kobertz, W. R.; Gonzalez-Scarano, F.; Bednarski, M. D. *J. Am. Chem. Soc.* **1992**, *114*, 10639.
(17) Kessler, H.; Wittmann, V.; Kock, M.; Kottenhahn, M. *Angew. Chem., Int. Ed. Engl.* **1992**, *31*, 902.
(18) Gurjar, M. K.; Mainkar, A. S.; Syamala, M. *Tetrahedron: Asymmetry* **1993**, *4*, 2343.
(19) Hofsteenge, J. H.; Müller, D. R.; de Beer, T.; Löffler, A.; Richter, W. J.; Vliegenthart, J. F. G. *Biochemistry* **1994**, *33*, 13524.
(20) Hoffman, M.; Kessler, H. *Tetrahedron Lett.* **1994**, *35*, 6067.
(21) Rassu, G.; Zanardi, F.; Battistini, L.; Casiraghi, G. *Tetrahedron: Asymmetry* **1995**, *6*, 371.
(22) Michael, K.; Wittmann, V.; Konig, W.; Sandow, J.; Kessler, H. *Int. J. Pept. Protein Res.* **1996**, *48*, 59.
(23) Grison, C.; Coutrot, F.; Coutrot, P. *Tetrahedron* **2001**, *57*, 6215.
(24) Grison, C.; Coutrot, F.; Coutrot, P. *Tetrahedron* **2002**, *58*, 2735.
(25) Coutrot, F.; Marraud, M.; Maigret, B.; Grison, C.; Coutrot, P. *Lett. Pept. Sci.* **2002**, *8*, 107.
(26) Coutrot, F. Ph.D. Thesis, Université Henri Poincaré − Nancy I, France, 2000.

10.1021/ja031778y CCC: $27.50

Scheme 1

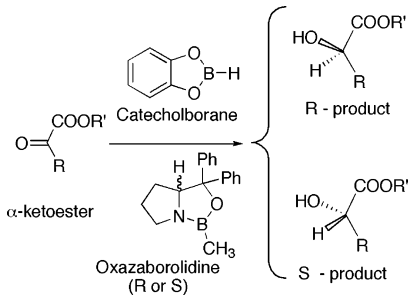

Scheme 2

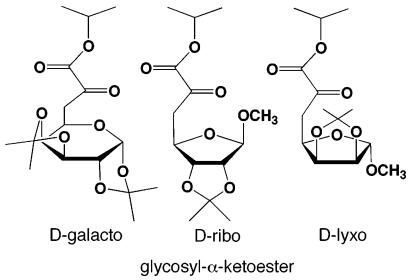

Table 1. Experimental Results for the Reduction of α-Ketoesters by Means of Catecholborane Assisted by a Chiral Oxazaborolidine Catalyst[24]

glycosyl α-ketoester	catalyst	yield, %	major product	de, %
D-ribo	S	61	R	70
	R	39	S	68
D-galacto	S	94	R	78
	R	81	S	90

very good diastereomeric excesses (de) have been achieved for the reduction of the α-ketoesters by means of the so-called CBS catalyst (or Corey−Bakshi−Shibata[27−29] catalyst). The general process is illustrated in Scheme 1, where R includes a D-galacto, D-ribo, or D-lyxo moiety shown in Scheme 2. Some experimental results are shown in Table 1 for isopropyl esters. The rationalization of these data is not straightforward, since both, the catalyst and the ketone, exhibit asymmetric centers and may contribute to the observed diastereomeric excess.

The reduction of carbonyl compounds with chiral oxazaborolidine catalysts has been widely investigated. This powerful synthetic method has been first reported by Itsuno et al.[30−36] and subsequently developed and rationalized by Corey and coworkers.[27−29,37−45] The mechanistic model proposed[28] assumes initial coordination of a borane (BH_3 for instance) to the Lewis basic nitrogen atom on the less hindered α face of the oxazaborolidine. This activates the borane as a hydride donor and also increases the Lewis acidity of the endocyclic boron atom. In a second step, the complex binds to the ketone at the more sterically accessible lone pair (i.e., syn with respect to the ketone substituent with the smaller effective steric bulk) and cis to the vicinal borane group. This aligns the carbonyl atom and the coordinated borane for face-selective hydride transfer via a six-membered transition structure to form the product. The mechanism is illustrated in Figure 1. The reaction finishes by regeneration of the catalyst.

Some difficulties arise if this scheme is used to rationalize the de observed in the case of the glycosyl α-ketoesters in Table 1. Indeed, if one considers that the glycosyl group is larger than the ester group, Corey's model would predict exactly the opposite diastereoselectivity to that found experimentally. Nevertheless, application of Corey's model to glycosyl α-ketoester reduction is not straightforward because asymmetric induction is not only connected to the chirality of the catalyst. The presence of chiral centers at the glycosyl group might play a role too so that the final de value should be a combination of both effects. Experimentally, the effect due to the catalyst and that due to the glycosyl group are not easily separable.

Theoretical computations on oxazaborolidine-catalyzed reduction of ketones have been reported by several authors. Most of the theoretical work has been carried out by Nevalainen.[46−64] Other contributions are due to Jones and Liotta,[65] Bach et al.,[66] Linney et al.,[67] Quallich et al.,[68] Bringmann et al.,[69,70] Göndös and Pálinkó,[71] and Li et al..[72−78] A thorough survey of all these

(27) Corey, E. J.; Bakshi, R. K.; Shibata, S. *J. Am. Chem. Soc.* **1987**, *109*, 5551.
(28) Corey, E. J.; Bakshi, R. K.; Shibata, S.; Chen, C. P.; Singh, V. K. *J. Am. Chem. Soc.* **1987**, *109*, 7925.
(29) Corey, E. J.; Bakshi, R. K.; Shibata, S. *J. Org. Chem.* **1988**, *53*, 2861.
(30) Itsuno, S.; Hirao, A.; Nakahama, S.; Yamazaki, N. *Macromol. Rapid Commun.* **1982**, *3*, 673.
(31) Itsuno, S.; Hirao, A.; Nakahama, S.; Yamazaki, N. *J. Chem. Soc., Perkin Trans. 1* **1983**, 1673.
(32) Itsuno, S.; Ito, K.; Hirao, A.; Nakahama, S. *J. Chem. Soc., Chem. Commun.* **1983**, 469.
(33) Itsuno, S.; Ito, K.; Hirao, A.; Nakahama, S. *J. Chem. Soc., Perkin Trans. 1* **1984**, 2887.
(34) Itsuno, S.; Ito, K.; Hirao, A.; Nakahama, S. *J. Org. Chem.* **1984**, *49*, 555.
(35) Itsuno, S.; Nakano, M.; Miyazaki, K.; Masuda, H.; Ito, K.; Hirao, A.; Nakahama, S. *J. Chem. Soc., Perkin Trans. 1* **1985**, 2039.
(36) Itsuno, S.; Nakano, M.; Ito, K.; Hirao, A.; Owa, M.; Kanda, N.; Nakahama, S. *J. Chem. Soc., Perkin Trans. 1* **1985**, 2615.
(37) Corey, E. J.; Link, J. O. *Tetrahedron Lett.* **1989**, *30*, 6275.
(38) Corey, E. J.; Chen, C. P.; Reichard, G. A. *Tetrahedron Lett.* **1989**, *30*, 5547.
(39) Corey, E. J. *European Pattern application*; Harvard College: USA Ep, 1989; p 29.
(40) Corey, E. J.; Bakshi, R. K. *Tetrahedron Lett.* **1990**, *31*, 611.
(41) Corey, E. J.; Link, J. O. *Tetrahedron Lett.* **1992**, *33*, 3431.
(42) Corey, E. J.; Link, J. O.; Bakshi, R. K. *Tetrahedron Lett.* **1992**, *33*, 7107.
(43) Corey, E. J.; Helal, C. J. *Tetrahedron Lett.* **1995**, *36*, 9153.
(44) Corey, E. J.; Helal, C. J. *J. Am. Chem. Soc.* **1997**, *118*, 111769.
(45) Corey, E. J.; Helal, C. J. *Angew. Chem., Int. Ed.* **1998**, *37*, 1986.
(46) Nevalainen, V. *Tetrahedron: Asymmetry* **1991**, *2*, 63.
(47) Nevalainen, V. *Tetrahedron: Asymmetry* **1991**, *2*, 429.
(48) Nevalainen, V. *Tetrahedron: Asymmetry* **1991**, *2*, 827.
(49) Nevalainen, V. *Tetrahedron: Asymmetry* **1991**, *2*, 1133.
(50) Nevalainen, V. *Tetrahedron: Asymmetry* **1992**, *3*, 1563.
(51) Nevalainen, V. *Tetrahedron: Asymmetry* **1992**, *3*, 1441.
(52) Nevalainen, V. *Tetrahedron: Asymmetry* **1992**, *3*, 921.
(53) Nevalainen, V. *Tetrahedron: Asymmetry* **1992**, *3*, 933.
(54) Nevalainen, V. *Tetrahedron: Asymmetry* **1993**, *4*, 1505.
(55) Nevalainen, V. *Tetrahedron: Asymmetry* **1993**, *4*, 1565.
(56) Nevalainen, V. *Tetrahedron: Asymmetry* **1993**, *4*, 1569.
(57) Nevalainen, V. *Tetrahedron: Asymmetry* **1993**, *4*, 1597.
(58) Nevalainen, V. *Tetrahedron: Asymmetry* **1994**, *5*, 289.
(59) Nevalainen, V. *Tetrahedron: Asymmetry* **1994**, *5*, 387.
(60) Nevalainen, V. *Tetrahedron: Asymmetry* **1994**, *5*, 395.
(61) Nevalainen, V. *Tetrahedron: Asymmetry* **1994**, *5*, 767.
(62) Nevalainen, V. *Tetrahedron: Asymmetry* **1994**, *5*, 903.
(63) Nevalainen, V.; Uggla, R.; Sundberg, M. R. *Tetrahedron: Asymmetry* **1995**, *6*, 1431.
(64) Nevalainen, V. *Tetrahedron: Asymmetry* **1996**, *7*, 2655.
(65) Liotta, D.; Jones, D. K. *Adv. Mol. Model.* **1995**, *3*, 1.
(66) Bach, J.; Berenguer, R.; Farras, J.; Garcia, J.; Meseguer, J.; Vilarrasa, J. *Tetrahedron: Asymmetry* **1995**, *6*, 2683.
(67) Linney, L. P.; Self, C. R.; Williams, I. H. *Tetrahedron: Asymmetry* **1994**, *5*, 813. Linney, L. P.; Self, C. R.; Williams, I. H. *J. Chem. Soc., Chem. Commun.* **1994**, 1651.
(68) Quallich, G. J.; Blake, J. F.; Woodall, T. M. *J. Am. Chem. Soc.* **1994**, *116*, 8516.
(69) Bringman, G.; Hinrichs, J. u.; Kraus, J. u.; Wuzik, A.; Schulz, T. *J. Org. Chem.* **2000**, *65*, 2517.
(70) Bringman, G.; Vitt, D. *J. Org. Chem.* **2000**, *65*, 2517.
(71) Göndös, G.; Pálinkó, I. *Int. J. Quantum Chem.* **2001**, *84*, 253.
(72) Li, M.; Xie, R. G.; Hu, C. W.; Wang, X.; Tian, A. M. *Int. J. Quantum Chem.* **2000**, *78*, 245.
(73) Li, M.; Xie, R. G.; Hu, X. R.; Tian, A. M. *Int. J. Quantum Chem.* **2000**, *78*, 261.
(74) Li, M.; Xie, R. G.; Tian, A. M. *Acta Chim. Sin.* **2000**, *58*, 510.
(75) Li, M.; Xie, R. G.; Tian, S. H.; Tian, A. M. *Int. J. Quantum Chem.* **2000**, *78*, 252.
(76) Li, M.; Tian, A. M. *THEOCHEM* **2001**, *544*, 25.

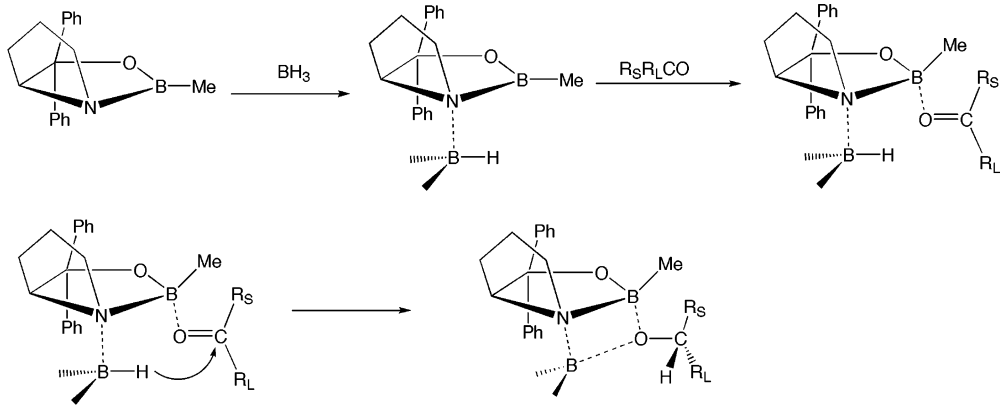

Figure 1. Mechanism proposed by Corey for the catalytic enantioselective reduction of ketones by oxazaborolidines. The R_S and R_L groups represent, respectively, the smaller and larger substituent groups of the ketone.

previous investigations has been recently reported by Alagona et al.[79] in this journal, and therefore we shall not comment on them in detail here (though some essential points are discussed below). In the work of Alagona et al., the authors have carried out ab initio density functional and semiempirical calculations for the system acetophenone + CBS catalyst + BH_3. The whole CBS catalyst is described in that work at the ab initio level for the first time, and many aspects of the reaction have been reexamined. It has been shown that the enantiomeric excess is controlled kinetically, and a pretty good agreement with experimental data for stereoselectivities has been obtained.

However, all these previous studies assume a nonchiral ketone, and therefore double asymmetric induction has not been accounted for. Besides, reduction of α-ketoesters with CBS catalysts has not yet been investigated in previous theoretical works. This has prompted us to perform the present theoretical study. Our aim is to analyze the role of different factors influencing diastereoselectivity in the reduction of glycosyl α-ketoesters by oxazaborolidine catalysts and to develop a model for the observed double asymmetric induction. The process considered here is the reduction of a D-galacto-α-ketoester. Several models of this reaction have been investigated.

2. Computational Method

Some previous theoretical studies on related systems have been carried out with semiempirical methods because they are much less costly than ab initio approaches and therefore permit the treatment of larger molecules. However, it has been shown that semiempirical methods can lead to erroneous conclusions in asymmetric synthesis studies[80−82] as far as some artifacts exist in the treatment of HH core−core interactions.[83−85] Moreover, the description of systems containing B atoms is rather poor at the semiempirical level. For instance, the complexation energy of $BH_3 + H_2CO$, which may be used to get a rough estimation of the catalyst−reactant interaction, is predicted to be −2.5 kcal/mol at the AM1 level, whereas ab initio calculations (MP2/6-311++G** level) lead to −15.2 kcal/mol. On the other hand, the recent study of Alagona et al.[79] has also shown that Hartree−Fock calculations are not reliable and that correlation energy must be taken into account. These authors have concluded that density functional theory (DFT) is a good compromise between accuracy and computational cost.[79] DFT calculations have also been carried out to analyze the coordination of aldehydes to oxazaborolidinones.[86] Considering the conclusions reached in these previous papers, the size of the systems considered in the present work and the large number of calculations required to analyze the various contributions to the selectivity, we have chosen to use a DFT method.

Our DFT computational scheme is based on the use of the B3LYP hybrid exchange-correlation functional[87,88] and the 6-31G* basis set[89−92] (a set of diffuse functions has been added for B atoms, as recommended in previous studies[93]). Full geometry optimizations have been performed for all the systems. Transition structures have been located and verified through frequency computations. Due to the large system size, study of the intrinsic reaction coordinate was not possible. However, the vibration mode corresponding to the imaginary frequency obtained in transition structure calculations was carefully analyzed. It always corresponds to the expected reaction path (hydride transfer). Zero-point energy (ZPE) corrections, as well as thermal corrections to the enthalpy and free energies, have been evaluated using standard approaches and the computed frequencies of vibration at the B3LYP level. All calculations have been carried out using Gaussian 98.[94]

3. Reaction Models and Notation

The main aim of our work has been to analyze the relative importance of the asymmetric induction arising from the catalyst structure and from the glucidic part on the reactant. To separate and analyze both effects, we have considered different models

(77) Li, M.; Tian, A. M. *THEOCHEM* **2001**, *544*, 37.
(78) Li, M.; Zheng, W. X.; Yang, F.; Tian, A. *Int. J. Quantum Chem.* **2001**, *81*, 291.
(79) Alagona, G.; Ghio, C.; Persico, M.; Tomasi, S. *J. Am. Chem. Soc.* **2003**, *125*, 10027. Alagona, G.; Ghio, C.; Tomasi, S. *Theor. Chem. Acc*. **2004**, in press
(80) Salvatella, L.; Mokrane, A.; Cartier, A.; Ruiz-López, M. F. *Chem. Phys. Lett.* **1998**, *296*, 239.
(81) Salvatella, L.; Mokrane, A.; Cartier, A.; Ruiz-López, M. F. *J. Org. Chem.* **1998**, *63*, 4664.
(82) Cativiela, C.; Dillet, V.; Garcia, J. I.; Mayoral, J. A.; Ruiz-López, M. F.; Salvatella, L. *THEOCHEM* **1995**, *331*, 37.
(83) Buss, V.; Messinger, J.; Heuser, N. *QCPE Bull.* **1991**, *11*, 5.
(84) Csonka, G. I. *J. Comput. Chem.* **1993**, *14*, 895.
(85) Csonka, G. I.; Angyan, J. G. *THEOCHEM* **1997**, *393*, 31.
(86) Salvatella, L.; Ruiz-López, M. F. *J. Am. Chem. Soc.* **1999**, *121*, 10772.
(87) Lee, C.; Yang, W.; Parr, R. G. *Phys. Rev. B* **1988**, *37*, 785.
(88) Becke, A. D. *J. Chem. Phys.* **1993**, *98*, 5648.
(89) Ditchfield, R.; Hehre, W. J.; Pople, J. A. *J. Chem. Phys.* **1971**, *54*, 724.
(90) Hehre, W. J.; Ditchfield, R.; Pople, J. A. *J. Chem. Phys.* **1972**, *56*, 2257.
(91) Dill, J. D.; Pople, J. A. *J. Chem. Phys.* **1975**, *62*, 2921.
(92) Hariharan, P. C.; Pople, J. A. *Theor. Chim. Acta* **1973**, *28*, 213.
(93) Tuñon, I. Ph.D. Thesis, University of Valencia, Spain, 1993.
(94) Frisch, M. J.; Trucks, G. W.; Schlegel, H. B.; Scuseria, G. E.; Robb, M. A.; Cheeseman, J. R.; Zakrzewski, V. G.; Montgomery, J. A., Jr.; Stratmann, R. E.; Burant, J. C.; Dapprich, S.; Millam, J. M.; Daniels, A. D.; Kudin, K. N.; Strain, M. C.; Farkas, O.; Tomasi, J.; Barone, V.; Cossi, M.; Cammi, R.; ennucci, B.; Pomelli, C.; Adamo, C.; Clifford, S.; Ochterski, J.; Petersson, G. A.; Ayala, P. Y.; Cui, Q.; Morokuma, K.; Salvador, P.; Dannenberg, J. J.; Malick, D. K.; Rabuck, A. D.; Raghavachari, K.; Foresman, J. B.; Cioslowski, J.; Ortiz, J. V.; Baboul, A. G.; Stefanov, B. B.; Liu, G.; Liashenko, A.; Piskorz, P.; Komaromi, I.; Gomperts; Martin, R. L.; Fox, D. J.; Keith, T.; Al-Laham, M. A.; Peng, C. Y.; Nanayakkara, A.; Challacombe, M.; Gill, P. M. W.; Johnson, B.; Chen, W.; Wong, M. W.; Andres, J. L.; Gonzalez, C.; Head-Gordon, M.; Replogle, E. S.; Pople, J. A. *Gaussian 98*, revision A.9 and A.11 ed.; Gaussian, Inc.: Pittsburgh, PA, 2001.

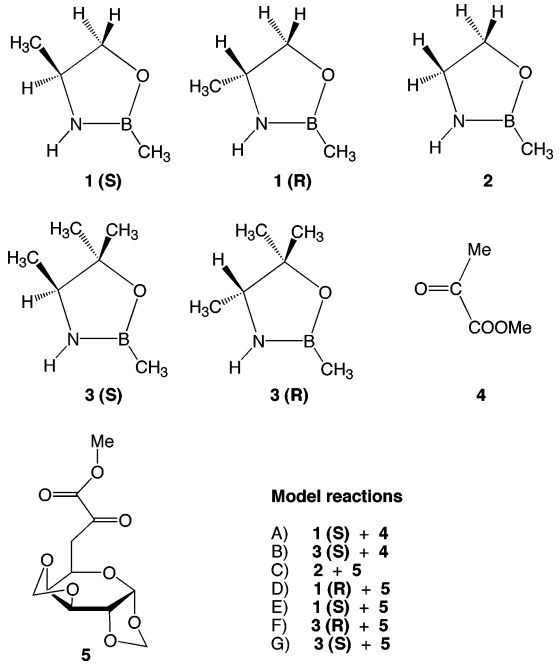

Figure 2. Model catalysts and ketoesters considered in this work.

of the reaction that are summarized in Figure 2. For the oxazaborolidine catalyst, we have considered three compounds: compound **1** represents the simplest model of a chiral oxazaborolidine catalyst, and **2** is a model for a nonchiral catalyst, whereas **3** is a chiral model that allows estimation of the influence of substituents on the C-5 atom at the oxazaborolodine ring. As shown, model reactions A−B correspond to the reaction of a simple nonchiral α-ketoester with a chiral catalyst model. In model C, we consider the reduction of the chiral glycosyl α-ketoester **5** with a nonchiral oxazaborolidine catalyst model. Finally, in models D−G, both the reactant and the catalyst are chiral, and we may examine the combined effect of the asymmetric groups. Note that compound **5** is close to the system studied experimentally (see Scheme 2), except that methyl groups have been replaced by hydrogen atoms.

In all reaction models, the hydrogen donor is BH_3. Replacing catecholborane by borane is not expected to modify much the results. This hypothesis has been confirmed by carrying out a series of preliminary semiempirical calculations.

The notation proposed in the original papers by Corey and co-workers for structures and conformations has been used throughout this paper, namely: the less (more) hindered face of the oxazaborolidine ring corresponds to the α (*β*) face, the small (R_S) and large (R_L) groups of the ketone correspond to the substituent with the smaller (larger) effective steric bulk, and catalyst−ketone complexes are assumed to have syn (anti) conformation when coordination to the oxygen occurs via the electron lone pair syn (anti) to the ketone substituent with the smaller steric bulk R_S (as shown in Figure 1).

It is important to stress that some authors[66,79] have used the opposite definition for syn/anti conformations, and particular attention should be paid to avoid confusion when comparing results in the literature. Besides, in the work of Alagona et al.,[79] the definition of small and large groups, R_S and R_L, has been done using the Cahn−Ingold−Prelog priority rules. In many cases, this is equivalent to the definition based on steric hindrance used in Corey's works. Using priority rules for assigning large and small groups makes the assignment of configuration in the product easier,[79] but in some cases, inconsistencies may arise. For instance, experimental de data reported by Corey and Helal[45] for the prochiral ketone Ph−CO−CH_2Cl is correctly predicted when one assumes R_L = Ph and R_S = CH_2Cl (see Table 5 in that paper). In contrast, use of Cahn−Ingold−Prelog priority rules in this case would lead to the opposite assignment of large and small substituents so that the wrong diastereoselectivity would be predicted.

Scheme 3

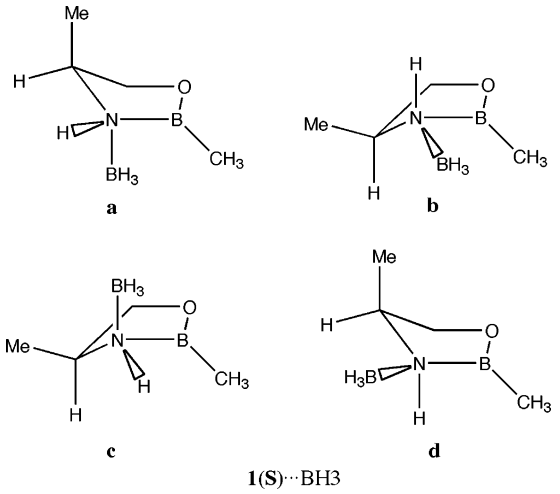

In this paper, we also use the notation "top" and "bottom" to differentiate the faces of the oxazaborolidine ring. When the ring is viewed as in Figure 2, the top face is that pointing toward the observer. According to this definition, structures in Figure 1, for instance, correspond to a bottom face attack. Note that the top (or bottom) face may correspond either to the less or to the more hindered face (α and *β* face, respectively). Finally, endo and exo conformations of the ketone coordinated to the oxazaborolidine have the usual meaning.

4. Results

4.1. Formation of Initial Catalyst−Borane Complexes. We first examine the formation of the initial oxazaborolidine−borane complexes. Several conformations of these complexes may be envisaged, although their relative energy may differ significantly. They are illustrated in Scheme 3 for the complex **1(S)**···BH_3. Structures **a** and **b** correspond to the attack through the bottom face of the ring (α attack in this case). Similarly, structures **c** and **d** correspond to the attack through the top face (*β* attack in this case). Geometry optimizations for these structures have shown that (1) **a** is the most stable one, (2) **b** is not an energy minimum, and (3) **d** lies 5.6 kcal/mol above **a** and 4.1 kcal/mol above **c**. Similar results are obtained for the other catalysts (in the case of catalyst **2**, structures **a** and **c** are isoenergetic). Thus, hereafter, we only consider the lowest structures of type **a** and **c**. Note that, in both cases, the borane lies in the axial position.

Table 2 summarizes the predicted formation energies for the oxazaborolidine−borane complexes. Table 3 gives some geometrical details, and Table 4 contains data on net atomic charges computed using the GhelpG method.[95]

(95) Breneman, C. M.; Wiberg, B. K. *J. Comput. Chem.* **1990**, *11*, 361.

Table 2. Energetics for the Catalyst−Borane Complex Formation (Energy Values in kcal/mol, Entropy Change in cal mol^{-1} K^{-1})

process	coordination	ΔE^{elec}	ΔE^{elec} + ZPE	ΔH (298 K)	$-\Delta S$	ΔG (298 K)
1 + BH_3	α-face	−23.80	−19.37	−20.64	40.1	−8.70
	β-face	−22.27	−17.64	−19.00	41.6	−6.58
2 + BH_3		−24.16	−19.70	−21.01	39.8	−9.14
3 + BH_3	α-face	−22.69	−18.26	−19.51	39.9	−7.60
	β-face	−21.68	−17.10	−18.41	41.4	−6.05

Table 3. Some Structural Parameters for BH_3, Catalysts, and Catalyst−Borane Complexes (Values in Å and Degrees)

compd	coordination	d_{NB} (endocyclic)	d_{NB} (exocyclic)	d_{BO}	d_{BH}	α_{BNB}
BH_3					1.193	
1		1.417		1.387		
2		1.417		1.387		
3		1.415		1.385		
1···BH_3	α-face	1.508	1.684	1.357	1.211	105.4
	β-face	1.510	1.684	1.358	1.211	104.2
2···BH_3		1.510	1.684	1.357	1.211	105.4
3···BH_3	α-face	1.504	1.687	1.352	1.211	107.6
	β-face	1.508	1.688	1.354	1.212	106.2

Table 4. Some Partial Atomic Charges for BH_3, Catalysts, and Catalyst−Borane Complexes (ChelpG Method)

		BH_3 unit	oxazaborolidine ring		
compd	coordination	B	N	B	O
BH_3		0.654			
1			−0.858	0.699	−0.526
2			−0.740	0.684	−0.483
3			−0.869	0.729	−0.604
1···BH_3	α-face	0.204	−0.072	0.550	−0.450
	β-face	0.238	−0.145	0.546	−0.468
2···BH_3		0.212	−0.030	0.537	−0.462
3···BH_3	α-face	0.239	−0.153	0.573	−0.541
	β-face	0.265	−0.224	0.576	−0.564

As shown, the free energy of complexation is close to 8−9 kcal/mol when the borane coordinates to the catalysts through the α-face. In the case of the chiral compounds **1** and **3**, coordination through the hindered *β*-face is, as expected, less favorable by roughly 2 kcal/mol. Our calculations are comparable to those reported in the recent work of Alagona et al..[79] These authors have considered a chiral oxazaborolidine with a fused ring similar to that shown in Scheme 1. Using data from their Table 2, one deduces that coordination through the less hindered face leads to a complexation energy of $\Delta E = -22.97$ kcal/mol and $\Delta G = -9.20$ kcal/mol, which are very close to the corresponding values obtained for our systems. Coordination of the borane through the hindered face is very unfavorable in the system investigated by Alagona et al. because of the presence of the proline ring that confers a high rigidity to the catalyst. The results reported by Quallich et al.[68] for related complexes predict about −27 to −28 kcal/mol for the complexation energy (less hindered face) using MP2/6-31G* energy calculations on Hartree−Fock optimized geometries.

As noted in previous studies,[47,68,79] after complexation, the endocyclic N−B (B−O) bond length increases (decreases) with respect to the free oxazaborolidine ring. This trend is sometimes interpreted as evidence for a partial *π*-character on the N−B and B−O bonds. After complexation with borane, the lone pair of the N atom in the ring cannot participate with the *π*-system and the N−B bond length increases. At the same time, the partial

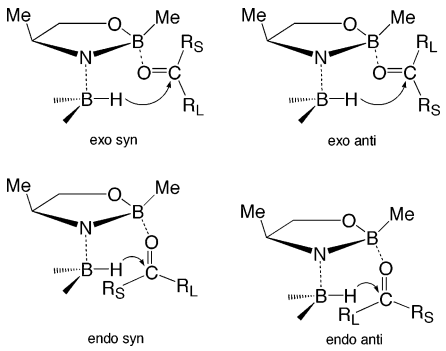

Figure 3. Possible coordination modes to model catalyst **1(S)** through the free α-face. The R_S and R_L groups represent respectively the smaller and larger substituent groups of the ketone.

π-character of the B−O bond is enhanced and the corresponding distance decreases. The net atomic charges in Table 4 shows that there is a huge electronic reorganization under the complexation process. This is a well-known phenomenon that explains the catalytic power of the oxazaborolidone ring as far as (1) it renders hydride transfer from the borane easier and (2) it enhances the Lewis acidity of the B atom in the ring. The computed exocyclic N···B bond length is very similar to that reported by Alagona et al. (1.680 Å) and is not far from the X-ray diffraction measurements by Corey et al. (1.62 Å).[42]

4.2. Formation of Catalyst−Borane−Ketone Complexes. The next step in the reaction mechanism proposed by Corey consists of the formation of a Lewis acid complex between the catalyst−borane adduct and the ketone. The complex involves the interaction between the oxazaborolidine-ring B atom and the O atom of the ketone. Depending on the coordination mode of the ketone, endo/exo and syn/anti conformations are expected. They are represented in Figure 3 in the case of an interaction through the less hindered face of the **1(S)** catalyst (α-face). As said above, the enantioselectivity of the reaction is generally explained by the preferential formation of the exo/syn complex which in principle minimizes steric interactions.

Several attempts to describe these complexes have been reported in the literature. In general, it has been shown that they are slightly stable or even unstable and that their predicted stability is very sensitive to the computational level. Nevalainen has discussed this question in several papers[47,57,63,64] finding unstable complexes in some cases[64] and slightly stable structures in others.[63] In the latter case, Hartree−Fock and MP2 calculations led to different conclusions. Stable complexes at the AM1 level have been described for instance by Williams et al..[67] Li and Tian[73,76,78] have described a complex among an oxazaborolidine derivative, BH_3, and 3,3-dimethyl-2-butanone at the Hartree−Fock 6-31G* level. From the four possible structures (endo/exo, syn/anti), only two of them (syn structures) led to energy minima, and the other two decomposed into a catalyst−borane adduct and ketone. Moreover, the syn complexes were shown to be less stable than the separated catalyst−borane complex and ketone, relative energies being 7.09 and 12.86 kcal/mol for the exo and endo configurations, respectively. No free energy computations were reported by these authors. In the same work, some structures at the B3LYP/6-31G* level were also described. Quallich et al.[68] have shown that Hartree−Fock results using the 3-21G basis set predict stable complexes although use of the more reliable 6-31G* basis set leads to dissociation. These authors have also carried out MP2/6-31G*

Figure 4. Catalyst−borane−ketone complex obtained with **1**···BH_3 + **4**.

computations on a model oxazaborolidine and have been able to locate endo and exo complexes. The relative energy with respect to the separated catalyst−BH_3 and ketone systems was particularly small: −0.52 kcal/mol and +0.46 kcal/mol, respectively. Most recent studies by Alagona et al.[79] have analyzed the influence of the computational level in some detail. In particular, they computed the potential energy surface at the AM1 level and performed further optimization calculations on AM1 minima using several ab initio and DFT approaches. They found, as in the work of Quallich et al.,[68] that Hartree−Fock with small basis sets (3-21G) predict local minima, whereas similar calculations with higher quality basis sets (6-31G*) do not. In contrast, they found two minima when using the B3LYP/6-31G* method corresponding to exo/anti and so-called skew/anti coordination of the ketone. The corresponding formation energies are positive, 2.19 and 1.97 kcal/mol, respectively (relative to separated ketone and oxazaborolidine−BH_3 complex). Free energies for these two complexes are rather high: 19.04 and 18.34 kcal/mol, respectively. The skew/anti coordination corresponds to a complex in which the C−B···O=C dihedral angle presents an unusual value, intermediate between the angle for pure endo and exo orientations (180° and 0°, respectively).

In line with these former investigations, our calculations have shown that complex formation is not a very favorable process. Thus, the **1**···BH_3 adduct does not form stable complexes with **5**. All geometry optimizations led to dissociation. The same adduct has been shown to form only one stable complex with the α-ketoester **4**, which does not correspond to standard endo or exo configurations. It is represented in Figure 4. The energy of this complex, relative to separated the **1**···BH_3 adduct and **4**, is positive, 4.5 kcal/mol, not far from the values given above from Alagona et al..[79] Its structure is not far from the skew complex described by these authors (C−B···O=C dihedral angle equal −102.2° vs −75.5° in ref 79). We have not computed the corresponding free energy, but one may expect a high value. Considering the previous reported results and those obtained in our work for **1**, no attempts have been made to locate energy minima with **2** and **3**.

Indeed, all these theoretical calculations suggest that the Lewis acidity of the oxazaborolidine B atom is much lower than expected and put a doubt on the role played by 3-fold complexes in the reduction process mechanism. Obviously, these remarks do not automatically apply for other reactions, since substituent effects may modify the stability of the complexes (for instance, we have found in exploratory calculations that the methyl group attached to the ring B atom plays a major role, stable complexes

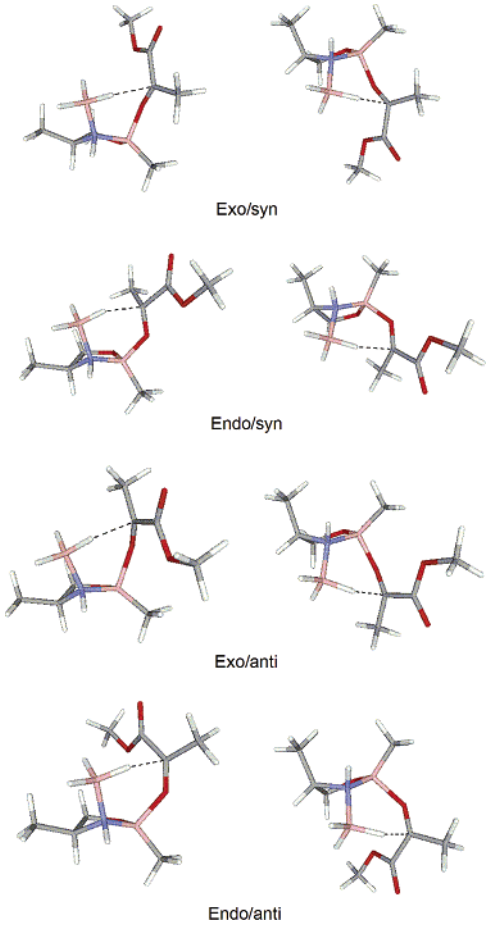

Figure 5. Transition structures for reaction A. Left: top attack. Right: bottom attack.

Table 5. Energies of Transition Structures Predicted for Model Reaction A: **1(S)** − BH_3 + **4** (in kcal/mol) (For **4**, Smaller and Larger Groups Are Assumed To Be R_S = CH_3 and R_L = COOMe

model reaction A: **1(S)** − BH_3 + **4**								
	top face (β-attack)				bottom face (α-attack)			
	exo/syn	endo/syn	exo/anti	endo/anti	exo/syn	endo/syn	exo/anti	endo/anti
conf[a]	S	R	R	S	R	S	S	R
ΔE^b	8.18	7.71	9.68	11.02	5.82	7.29	7.51	9.32
$\delta\Delta E$	2.36	1.89	3.86	5.20	0.00	1.47	1.69	3.50
ΔG^b	24.14	24.09	24.87	27.02	21.42	23.34	22.87	24.94
$\delta\Delta G$	2.72	2.67	3.45	5.60	0.00	1.92	1.45	3.52

[a] Absolute configuration of the obtained product. [b]With respect to separated catalyst−borane complex and ketoester.

being obtained when such a group is replaced by a hydrogen atom). Definitive conclusions on this point would therefore require a larger study and higher computational levels.

It may be useful to make a comment on the interaction of a simple borane like BH_3 with a carbonyl compound. In principle, such an interaction leads to much higher interaction energies than those obtained for the oxazaborolidines. Ab initio computations for the simple system H_2CO···BH_3[96] leads to a coordination energy of −17.1 kcal/mol (using the B3LYP level employed in our work, one obtains −18.06 kcal/mol). Luque et al.[97] have reported a DFT study on HCOOR···BH_3, but they have focused on complex conformations vs solvent effect. We have computed

(96) Le Page, T. J.; Wiberg, B. K. *J. Am. Chem. Soc.* **1988**, *110*, 6642.
(97) Luque, F. J.; Cossi, M.; Tomasi, J. *THEOCHEM* **1996**, *371*, 123.

Table 6. Some Geometrical Parameters of Transition Structures Predicted for Model Reaction A: **1(S)** − BH_3 + **4** (in Å and Degrees) (For **4**, Smaller and Larger Groups Are Assumed To Be R_S = CH_3 and R_L = COOMe)[a]

	model reaction A: **1(S)** − BH_3 + **4**							
	top face (β-attack)				bottom face (α-attack)			
	exo/syn	endo/syn	exo/anti	endo/anti	exo/syn	endo/syn	exo/anti	endo/anti
$B_2\cdots H$	1.230	1.226	1.232	1.226	1.233	1.231	1.239	1.235
$H\cdots C_2$	2.445	2.353	2.126	2.217	2.193	2.200	2.543	2.022
C_2O_1	1.238	1.240	1.237	1.236	1.238	1.241	1.242	1.240
NB_1	1.607	1.605	1.603	1.600	1.601	1.605	1.605	1.596
NB_2	1.635	1.635	1.627	1.629	1.632	1.637	1.620	1.627
$O_1\cdots B_1$	1.704	1.625	1.765	1.739	1.710	1.650	1.742	1.766
$C_2O_1B_1$	133.6	131.7	139.7	139.4	132.6	131.2	138.5	138.5
$C_2O_1B_1C_1$	−57.40	170.3	−80.0	−158.8	58.2	−178.9	86.8	139.0
$C_4C_2O_1B_1$	40.6	−30.2	−135.6	142.1	−44.6	38.4	133.3	−128.5
$O_2C_3C_2O_1$	178.9	178.8	169.80	171.9	−179.7	−169.6	−167.6	−179.3

[a] For the geometrical parameters considered in this table, see Scheme 4.

the interaction energy for the system **4**$\cdots BH_3$ which is −16.4 kcal/mol or −15.4 kcal/mol, depending if the coordination of BH_3 to the oxygen atom is syn or anti with respect to the methyl group. It may be also interesting to note that the geometry of the ketoester, in particular, the OCCO dihedral angle, is quite sensitive to the interaction with the borane. Whereas in the syn complex the angle is close to 180° (like in the free ketoester), in the anti complex the angles decreases to 103.7°. We shall see later that this angle plays a key role on the relative stabilization of transition structures.

4.3. Transition Structures for Hydride Transfer. To analyze the main factors determining the asymmetric induction in the hydrogenation process, the structure and relative energy of transition structures for hydride transfer have to be considered. In principle, for a chiral catalyst (model systems **1** and **3**), eight transition structures might be envisaged. They correspond to attacks through the α- and β-faces of the catalyst (free and hindered face, respectively) and to endo/exo and syn/anti orientations of the ketone (see Figure 3). For nonchiral catalysts (like **2**), the two faces of the oxazaborolidine ring are equivalent. However, if the ketone is chiral (like **5**), attacks through top and bottom faces (see Scheme 3) are not equivalent and eight structures have to be inspected in this case too. According to Corey's model, α-exo transition structures are favored for steric reasons and asymmetric induction would be related to an energy difference between syn/anti transition states.

We present now the results obtained for the model reactions described in Figure 2. The discussion starts by considering reactions A−B, which involve a chiral catalyst and a simple nonchiral α-ketoester. Then, we shall consider reaction C, which involves a nonchiral catalyst and a model glycosyl α-ketoester. Finally, reactions D−G, in which a glycosyl α-ketoester is reduced by a chiral catalyst, will be studied.

As shown in Figure 1, Corey's model assumes that the transition structures for hydride transfer are characterized by the formation of a six-membered ring. The conformation of the cycle has been the object of some discussion in the literature. Both chairlike and boatlike conformations have been obtained[65,67−69,79] depending on system, endo/exo orientation, and calculation levels. In the case of the reactions with the nonchiral ketoester **4**, our results predict chairlike conformations for endo TSs and twist-boat conformations for the exo ones, although one should notice that all conformations are quite distorted (see Supporting Information). In the case of the reaction with the glycosyl α-ketoester **5**, the results are a little different. Most of TS geometries exhibit a twist-boat conformation, and only a few may be described as chairlike conformations. The latter correspond to either endo or exo orientations, but their conformation is always anti. Attempts to locate several types of structure for a given TS were made in a few cases, but results were unfruitful. The previous trends present some discrepancies with some of the studies cited above, particularly with those of Quallich et al.[68] and Alagona et al.,[79] who employed a comparable theoretical level, suggesting that the nature of the reactant plays a decisive role on TS ring conformation.

A. Reactions Involving a Chiral Oxazaborolidine and a Nonchiral α-Ketoester. Reactions A and B (see Figure 2) have been selected to evaluate the asymmetric induction of the catalyst on the reduction of an α-ketoester. The catalysts are assumed to have (S) configuration. The eight possible transition structures have been located. They are represented in Figure 5. The energetics and structural parameters are summarized in Tables 5 and 6, respectively. Note that, for the α-ketoester considered here, compound **4**, we assume the smaller and larger groups to be R_S = CH_3 and R_L = COOMe. Syn and anti orientations are defined accordingly.

As shown, the predictions are in good agreement with Corey's model: (*S*)-oxazaborolidine favors the TS corresponding to α-attack and exo/syn orientation of the ketone, this TS leading to R product. One may note also the following points: (1) For a given ketoester orientation, α attack is favored. (2) In general, exo structures are preferred to the corresponding endo ones (except for β syn attack, both structures, endo and exo, having a comparable energy). (3) Syn orientation is always preferred to anti orientation. (4) Activation free energies are in the range 21−27 kcal/mol in close agreement with results from Alagona et al.[79] for the reaction acetophenone + CBS + BH_3 (for instance, the exo/anti pathway displays a barrier of 22.51 kcal/mol at the B3LYP). And, (5) the most stable TS leading to the S product configuration displays exo/anti structure and is 1.45 kcal/mol over the exo/syn TS.

One may see in Table 6 that the geometry of these transition structures displays some significant differences (see Scheme 4 for definition of the parameters). The length of the forming CH bond varies from 2.022 Å (α-endo/anti) to 2.543 Å (α-exo/anti). The O$\cdots$B bond length is also quite dependent on TS and varies in the range 1.650−1.766 Å. The length of the bond being broken, BH, is in all cases close to 1.23 Å, whereas that of the ketone CO bond is about 1.24 Å. It is interesting to remark that the dihedral angle $C_2O_1B_1C_1$ displays values that in some

Scheme 4

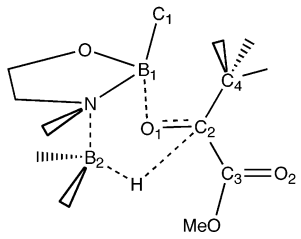

Table 7. Energies of Transition Structures Predicted for Model Reaction B: **3(S)** − BH_3 + **4** (in kcal/mol) (For **4**, Smaller and Larger Groups Are Assumed To Be R_S = CH_3 and R_L = COOMe)

model reaction B: **3(S)** − BH_3 + **4**								
	top face (β-attack)				bottom face (α-attack)			
	exo/syn	endo/syn	exo/anti	endo/anti[c]	exo/syn	endo/syn	exo/anti	endo/anti[c]
conf[a]	S	R	R	S	R	S	S	R
ΔE[b]	8.06	9.51	10.31		6.57	9.32	8.90	
$\delta\Delta E$	1.49	2.94	3.75		0.00	2.77	2.33	
ΔG[b]	24.27	25.98	25.74		22.52	25.6	24.55	
$\delta\Delta G$	1.75	3.46	3.22		0.00	3.08	2.02	

[a] Absolute configuration of the obtained product. [b]With respect to separated catalyst−borane complex and ketoester. [c]TS not found.

cases are far from those expected for "pure" endo or exo structures (180° and 0°, respectively). For instance, in some exo conformations, the angle is close to 90° corresponding to an intermediate endo/exo orientation. For simplicity, we still call them "exo" TSs (the absolute value of the angle being less than 90°), but our results clearly show that the classification of TSs as endo or exo may be somewhat arbitrary. A similar remark can be made for syn/anti orientation. For example, in the α-endo/syn TS, the $C_2O_1B_1C_1$ atoms are almost coplanar, whereas the $C_4C_2O_1B_1$ dihedral angle (38.4°) is quite different from that corresponding to a "pure" syn orientation (0°). This is related to the skew-type conformations reported by Alagona et al..[79]

Finally, one may note that the $O_2C_3C_2O_1$ angle is in most cases close to 180° although, for some structures, steric interactions give rise to a rotation around the CC bond (about 10°) decreasing the stabilization through π-resonance of CO bonds.

Let us now consider the model reaction B: **3(S)** − BH_3 + **4**. Compound **3** is similar to compound **1** in reaction A but differs from it by the presence of two methyl groups attached to the oxazaborolidine ring at C-5. The comparison of reactions A and B allows evaluation of the substituent effect on the reactivity

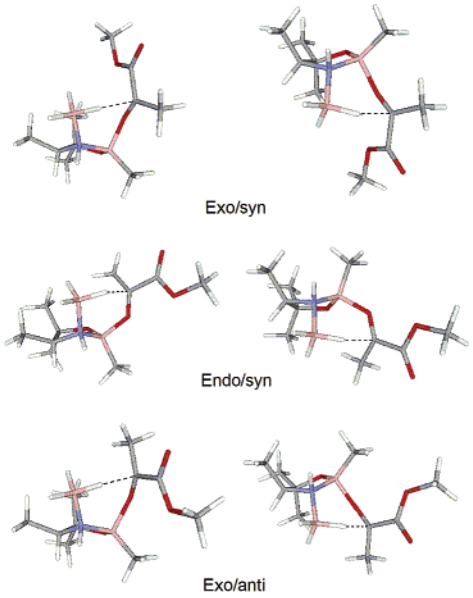

Figure 6. Transition structures for reaction B. Left: top attack. Right: bottom attack.

and selectivity properties of the catalyst. The results are presented in Tables 7 and 8 for energy and geometry results, respectively. The structures are drawn in Figure 6. In this case, endo/anti conformations have not been located despite a careful exploration of the potential energy surface in the vicinity of such hypothetic transition structures. For the remaining six structures, the results are comparable to those obtained in reaction A. In particular, the catalyst exhibits the same selectivity (R product favored), and the most stable TS corresponds to α-exo/syn attack. However, in contrast to reaction A, the most stable TS leading to S product has β-exo/syn conformation (instead of α-exo/anti in reaction A). Besides, one may note that the predicted selectivity is slightly larger in reaction B, since the free energy difference between the most stable TSs leading to R and S configurations of the product is now 1.75 kcal/mol. The free energy of activation is now in the range 22−26 kcal/mol roughly, and for a given TS type, it is slightly higher than in reaction model A.

B. Reactions Involving a Nonchiral Oxazaborolidine and a Glycosyl α-Ketoester. Reaction C (see Figure 2) is suitable to examine the asymmetric induction arising from the chirality of the pyranosyl group of the α-ketoester. Again, there are eight possible transition structures. All them have been located and

Table 8. Some Geometrical Parameters of Transition Structures Predicted for Model Reaction B: **3(S)** − BH_3 + **4** (in Å and Degrees) (For **4**, Smaller and Larger Groups Are Assumed To Be R_S = CH_3 and R_L = COOMe)[a]

model reaction B: **3(S)** − BH_3 + **4**								
	top face (β-attack)				bottom face (α-attack)			
	exo/syn	endo/syn	exo/anti	endo/anti[b]	exo/syn	endo/syn	exo/anti	endo/anti[b]
$B_2\cdots H$	1.234	1.227	1.240		1.236	1.230	1.242	
$H\cdots C_2$	2.149	2.384	2.019		2.114	2.284	1.994	
C_2O_1	1.239	1.239	1.243		1.241	1.242	1.244	
NB_1	1.601	1.600	1.604		1.594	1.597	1.595	
NB_2	1.633	1.635	1.621		1.629	1.632	1.618	
$O_1\cdots B_1$	1.718	1.617	1.736		1.718	1.615	1.751	
$C_2O_1B_1$	132.00	132.70	137.40		131.28	131.89	135.16	
$C_2O_1B_1C_1$	−58.80	171.90	−82.80		59.80	−176.65	75.90	
$C_4C_2O_1B_1$	−30.6	47.6	−133.6		−48.82	36.7	135.1	
$O_2C_3C_2O_1$	179.02	173.40	174.30		178.40	171.60	173.60	

[a] For the geometrical parameters considered in this table, see Scheme 4. [b]TS not found.

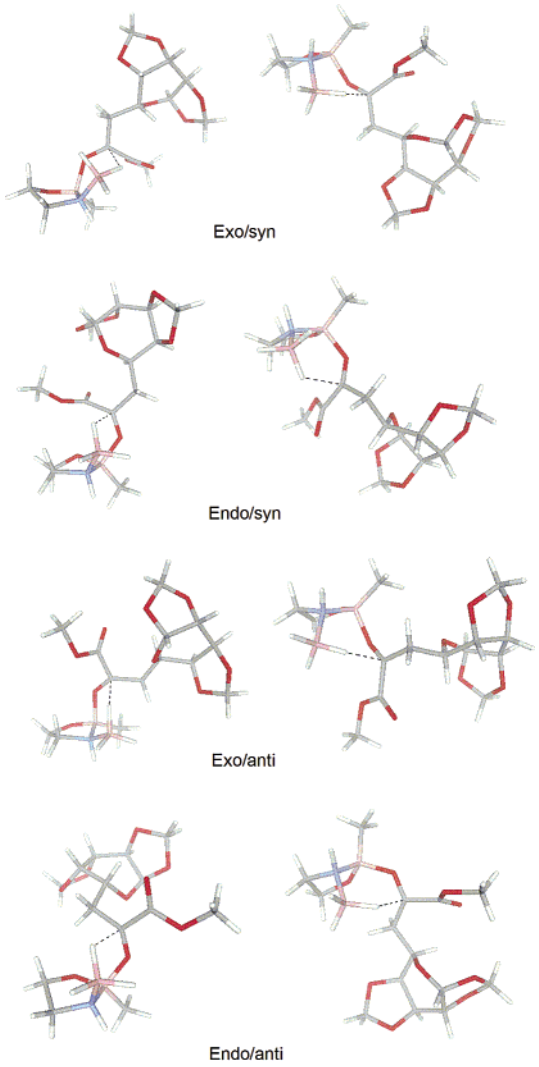

Figure 7. Transition structures for reaction C. Left: top attack. Right: bottom attack.

Table 9. Energies of Transition Structures Predicted for Model Reaction C: **2** − BH_3 + **5** (in kcal/mol) (For **5**, Smaller and Larger Groups Are Assumed To Be R_S = COOMe and R_L = Pyranosyl Group)

model reaction C: **2** – BH_3 + **5**								
	top face				bottom face			
	exo/syn	endo/syn	exo/anti	endo/anti	exo/syn	endo/syn	exo/anti	endo/anti
conf[a]	R	S	S	R	S	R	R	S
ΔE^b	5.68	5.19	5.44	4.2	6.24	6.67	4.84	7.87
$\delta\Delta E$	1.48	0.99	1.25	0.00	2.04	2.47	0.64	3.67
ΔG^b	22.02	22.15	21.59	19.88	22.37	21.78	20.24	24.48
$\delta\Delta G$	1.14	2.27	1.71	0.00	2.49	1.90	0.36	4.60
$\delta\Delta G^c$					2.13	1.54	0.00	4.24

[a] Absolute configuration of the obtained product. [b] With respect to separated catalyst−borane complex and ketoester. [c] Relative energy with respect to the exo/anti bottom face attack.

are drawn in Figure 7. The corresponding energetics and structural parameters are summarized in Tables 9 and 10. Note that, for α-ketoester **5**, syn/anti orientation is defined assuming that the smaller and larger substituents are R_S = COOMe and R_L = pyranosyl group.

Compared to the previous reactions A and B, which presents the expected behavior of Corey's model, reaction C displays some noteworthy features. First, the most stable TS does not correspond to exo/syn orientation of the ketone but to endo/anti one (top attack). The difference between the two conformations is however not very large (1.14 kcal/mol). Both lead to product R. One should note that, among the other TSs, there is one (exo/anti bottom face attack) which is rather stable. It also leads to R product. For convenience, we have also included in Table 9 the relative energy of bottom attack TSs with respect to that TS. Indeed, it is interesting to compare these values with those obtained for the bottom attack in model reaction A. The predicted R/S product selectivity is comparable showing that the influence of the methyl group at the C-4 atom of the ring is not very large, except of course that it enforces the attack through the less hindered face.

In model reaction C, the lowest TS leading to S product corresponds to the exo/anti top face attack, and it lies 1.71 kcal/mol above the most stable TS. Therefore, our calculations predict the formation of a major quantity of product with R configuration, as in the case of reactions A and B. Besides, the diastereomeric excess induced by the chiral structure of the pyranosyl group appears to be comparable to that of the oxazaborolidine models in reactions A or B.

As far as geometry parameters are concerned, the most interesting result for this reaction is the value of the $O_2C_3C_2O_1$ dihedral angle (Scheme 5). This angle is 146° in the free ketoester **5** but changes substantially under TS formation. In the case of endo/syn top face attack, it amounts to −81.1°. One may note that for the most stable TSs, the angle is not far from 180° (note also that, in a simple α-ketoester like **4**, the equilibrium angle is 180° as said above).

Although there is not an evident correlation between the value of the $O_2C_3C_2O_1$ dihedral angle and the relative stability of the TS, the analysis of the results suggests a possible explanation for the unexpected syn vs anti conformation stability of some TSs in this reaction. For a "pure" syn orientation, the ester group interacts repulsively with the catalyst, as seen in Scheme 6. To minimize these interactions, the $O_2C_3C_2O_1$ dihedral angle must change, but the loss of planarity involves a decrease of the stabilizing energy due to delocalization in the π-system. In other words, the ketoester group exhibits a poor flexibility and "pure" syn conformations are expected to be little stable. In contrast, in anti orientation, rotation around the CC bond is easy allowing the large sugar group to lie as far away as possible from the catalyst (see Scheme 7). Obviously, this is an oversimplified picture, since rotation around the B···O bond is also possible, but our DFT calculations clearly indicate that syn orientation for the ester group is unfavored.

C. Reactions Involving a Chiral Oxazaborolidine and a Glycosyl α-Ketoester. Reactions D−G (see Figure 2) are now taken into account. The asymmetric induction is in this case due to a combined effect of the catalyst and the glycosyl group. For simplicity, and considering the results presented above for reactions A−B, we only consider now the transition structures corresponding to the attack through the less hindered α-face of the catalyst. This corresponds to the top (bottom) face of the oxazaborolidine ring in the case of the R (S) configuration of the catalyst. For each reaction, four transition structures have been searched.

We discuss first the results obtained for reactions D and E. The located TSs are shown in Figure 8. Results for energetics and structural parameters are summarized in Tables 11 and 12.

Table 10. Some Geometrical Parameters of Transition Structures Predicted for Model Reaction C: **2** − BH_3 + **5** (in Å and Degrees) (For **5**, Smaller and Larger Groups Are Assumed To Be R_S = COOMe and R_L = Pyranosyl Group)[a]

	model reaction C: **2** – BH_3 + **5**							
	top face				bottom face			
	exo/syn	endo/syn	exo/anti	endo/anti	exo/syn	endo/syn	exo/anti	endo/anti
$B_2\cdots H$	1.231	1.236	1.239	1.248	1.266	1.246	1.235	1.234
$H\cdots C_2$	2.201	2.178	2.049	2.019	2.231	1.981	2.157	2.086
C_2O_1	1.242	1.252	1.250	1.247	1.244	1.243	1.238	1.254
NB_1	1.605	1.612	1.591	1.624	1.606	1.600	1.617	1.613
NB_2	1.627	1.618	1.608	1.621	1.631	1.605	1.627	1.634
$O_1\cdots B_1$	1.695	1.586	1.695	1.615	1.668	1.688	1.672	1.589
$O_2\cdots H$	2.569	2.504	2.375	2.461	2.524	2.416	2.592	2.401
$C_2O_1B_1$	130.2	126.1	131.1	129.7	131.1	137.0	132.5	128.9
$C_2O_1B_1C_1$	−52.0	171.9	−61.0	171.7	54.5	148.6	58.0	−173.7
$C_3C_2O_1B_1$	39.26	−38.4	−156.35	150.0	−40.1	57.5	150.4	149.4
$O_2C_3C_2O_1$	−116.6	−81.1	−107.7	−176.6	−87.5	−172.9	171.1	−103.6
$C_5C_4C_2O_1$	177.0	150.7	172.3	−106.8	154.9	−114.3	−97.4	168.7
$O_1C_2C_4C_5$	71.6	66.9	56.0	148.5	66.1	41.9	56.9	57.7

[a] For the geometrical parameters considered in this table, see Scheme 5.

Scheme 5

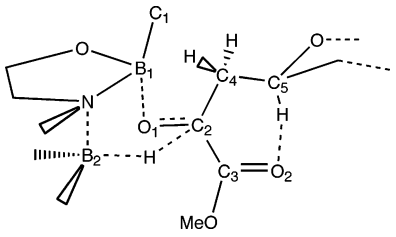

Scheme 6

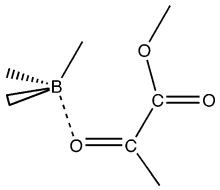

Scheme 7

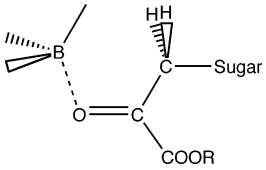

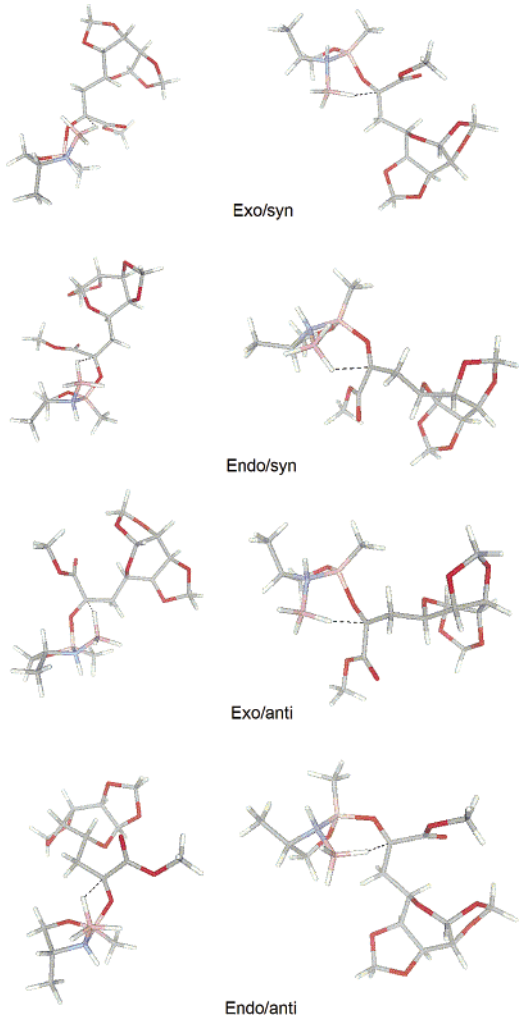

Figure 8. Transition structures for reactions D (left) and E (right). Only the attack through the less hindered α-face is considered for these reactions.

Qualitatively, results are not very different from those found for reaction C above, if one compares the free energy obtained for the top and bottom attack in reaction C with those obtained for reactions **1(R)** and **1(S)** catalysts, respectively. Indeed, the processes are very similar, the only difference being the presence of the methyl group on the oxazaborolidine ring. In reaction D (top face attack assumed), the lowest TS has endo/anti orientation, like in the top face attack of reaction C. In reaction E (bottom face attack assumed), the lowest TS has exo/anti orientation, like in the bottom face attack of reaction C. These TSs evolve to the R product. One must note however that, in reaction D, the electronic energy of the endo/syn TS, which leads to S product, is very slightly lower than that of the endo/anti TS, the latter becoming more stable when free energy is considered.

Let us consider now reactions F and G. As in the case of reaction B in which catalyst **3** is also involved, endo/syn transition structures have not been located despite several trial calculations. The obtained structures are in Figure 9, and the results for energy and geometries are in Tables 13 and 14.

The computations predict now the S product for reaction F (R catalyst) and the R product for reaction G (S catalyst). In both reactions, the lowest TSs involve exo/anti orientation of the ketoester. That is, the large pyranosyl group is oriented toward the B-Me unit (anti orientation), in contrast to Corey's

Table 11. Energies of Transition Structures Predicted for Model Reactions D and E: **1(R** or **S)** − BH_3 + **5** (in kcal/mol) (For **5**, Smaller and Larger Groups Are Assumed To Be R_S = COOMe and R_L = Pyranosyl Group)

	model reaction D: **1(R)** – BH_3 + 5				model reaction E: **1(S)** – BH_3 + 5			
	top face (α-attack)				bottom face (α-attack)			
	exo/syn	endo/syn	exo/anti	endo/anti	exo/syn	endo/syn	exo/anti	endo/anti
conf[a]	R	S	S	R	S	R	R	S
ΔE[b]	6.17	4.96	5.75	5.18	6.79	6.66	5.38	9.91
$\delta\Delta E$	1.22	0.00	0.80	0.23	1.41	1.28	0.00	4.53
ΔG[b]	22.55	21.67	21.79	21.05	22.82	21.86	20.8	26.83
$\delta\Delta G$	1.50	0.62	0.74	0.00	2.01	1.06	0.00	6.03

[a] Absolute configuration of the obtained product. [b]With respect to separated catalyst−borane complex and ketoester.

model but in line with the structures presented above for other reactions. The energy difference between the lowest TSs leading to R and S product configurations is 2.92 kcal/mol in the case of reaction F and 1.24 kcal/mol in the case of reaction G. This model predicts therefore a higher selectivity for the catalyst with R configuration.

4.4. Oxazadiboretane Intermediate Products. The formation of an oxazadiboretane intermediate product (see Scheme 8) was predicted in Corey's model[45] and has been experimentally observed through low-temperature NMR investigations.[99] Besides, this intermediate has been described in a number of theoretical calculations.[49,52,67,75,76] Dissociation to regenerate the catalyst and form an alkoxyborane may occur by two different reaction mechanisms: cycloelimination or borane addition. In the second case, a six-membered bridged species is formed that decomposes to the catalyst−borane complex and the alkoxyborane.

To obtain an estimation of the reaction energy, we have carried out computations for this intermediate. Nevertheless, considering that the present study focuses on diastereofacial selectivity, only the case of reaction A has been taken into account. A total number of four structures have been obtained corresponding to attack through the most favorable α-face. The newly created chiral center may have R or S configuration and, for each one, endo and exo conformations have been found. They are drawn in Figure 10 for the R product, and Table 15 summarizes their main geometrical parameters. Relative energy with respect to the separated reactants (**1(S)**−BH_3 + **4**) is very

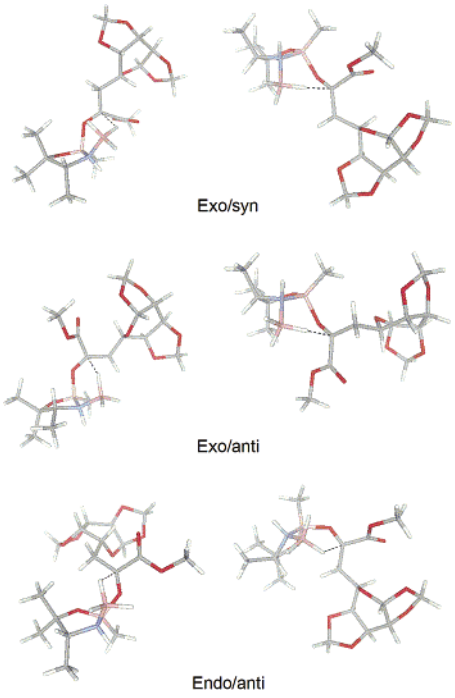

Figure 9. Transition structures for reactions F (left) and G (right). Only the attack through the less hindered α-face is considered for these reactions.

close for the four intermediate products: −38.3 kcal/mol (R, exo), −38.7 kcal/mol (R, endo), −38.9 (S, exo and endo). Free energy amounts are −19.3 and −19.5 kcal/mol for the R product exo and endo structures, respectively (thermochemistry calculations were not carried out for the S product but similar results are expected). Therefore, in agreement with previous calculations reported in the literature, we predict a highly exothermic process. For comparison, the study by Alagona et al. led to ΔG = −22.41 kcal/mol.

4.5. Discussion on the Double Asymmetric Induction. Table 16 summarizes the predicted diastereomeric excess for the different reactions considered in this work. In all cases, all the computed transition structures have been taken into account, and a Boltzmann weighted distribution has been considered. Two main points may be noted. First, reactions A and B show that chiral oxazaborolidines with S configuration lead to a main product displaying R configuration (likewise R oxazaborolidines

Table 12. Some Geometrical Parameters of Transition Structures Predicted for Model Reactions D and E: **1(R** or **S)** − BH_3 + **5** (in Å and Degrees) (For **5**, Smaller and Larger Groups Are Assumed To Be R_S = COOMe and R_L = Pyranosyl Group)[a]

	model reaction D: **1(R)** – BH_3 + **5**				model reaction E: **1(S)** – BH_3 + **5**			
	top face (α-attack)				bottom face (α-attack)			
	exo/syn	endo/syn	exo/anti	endo/anti	exo/syn	endo/syn	exo/anti	endo/anti
$B_2\cdots H$	1.232	1.234	1.238	1.243	1.228	1.244	1.237	1.234
$H\cdots C_2$	2.169	2.200	2.048	2.077	2.194	1.987	2.118	2.041
C_2O_1	1.243	1.251	1.250	1.245	1.245	1.242	1.240	1.254
NB_1	1.603	1.608	1.591	1.625	1.604	1.597	1.616	1.615
NB_2	1.624	1.620	1.611	1.617	1.629	1.624	1.607	1.641
$O_1\cdots B_1$	1.693	1.589	1.697	1.609	1.666	1.695	1.685	1.604
$O_2\cdots H$	2.553	2.499	2.374	2.446	2.522	2.409	2.624	2.400
$C_2O_1B_1$	129.7	126.3	131.4	129.7	130.6	136.6	132.0	129.4
$C_2O_1B_1C_1$	−52.3	170.7	−60.3	168.0	54.9	149.8	58.0	−176.8
$C_3C_2O_1B_1$	40.8	−37.4	152.2	148.2	−41.6	55.9	149.8	−167.5
$O_2C_3C_2O_1$	−119.0	−86.6	−107.6	−176.6	−85.9	−171.5	176.6	−101.3
$C_5C_4C_2O_1$	179.3	151.1	172.4	−106.8	152.7	−116.1	−95.2	165.5
$O_1C_2C_4C_5$	71.8	67.6	55.6	48.6	67.0	42.2	58.3	50.0

[a] For the geometrical parameters considered in this table, see Scheme 5.

Table 13. Energies of Transition Structures Predicted for Model Reactions F and G: **3(R** or **S)** − BH_3 + **5** (in kcal/mol) (For **5**, Smaller and Larger Groups Are Assumed To Be R_S = COOMe and R_L = Pyranosyl Group)

	model reaction F: **3(R)** − BH_3 + **5**				model reaction G: **3(S)** − BH_3 + **5**			
	top face (α-attack)				bottom face (α-attack)			
	exo/syn	endo/syn[c]	exo/anti	endo/anti	exo/syn	endo/syn[c]	exo/anti	endo/anti
conf[a]	R	S	S	R	S	R	R	S
ΔE[b]	7.15		5.04	7.65	7.83		6.30	7.07
δΔE	2.11		0.00	2.51	1.53		0.00	0.77
ΔG[b]	23.59		20.67	23.59	24.55		22.40	23.64
δΔG	2.92		0.00	2.92	2.15		0.00	1.24

[a] Absolute configuration of the obtained product. [b]With respect to separated catalyst−borane complex and ketoester. [c]TS not found.

Table 14. Some Geometrical Parameters of Transition Structures Predicted for Model Reactions F and G: **3(R** or **S)** − BH_3 + **5** (in Å and Degrees) (For **5**, Smaller and Larger Groups Are Assumed To Be R_S = COOMe and R_L = Pyranosyl Group)

	model reaction F: **3(R)** − BH_3 + **5**				model reaction G: **3(S)** − BH_3 + **5**			
	top face (α-attack)				bottom face (α-attack)			
	exo/ syn	endo/ syn[b]	exo/ anti	endo/ anti	exo/ syn	endo/ syn[b]	exo/ anti	endo/ anti
$B_2\cdots H$	1.235		1.238	1.245	1.231		1.240	1.240
$H\cdots C_2$	2.122		2.032	2.074	2.132		2.067	2.081
C_2O_1	1.244		1.249	1.245	1.247		1.241	1.251
NB_1	1.595		1.587	1.614	1.597		1.07	1.606
NB_2	1.623		1.618	1.623	1.627		1.623	1.623
$O_1\cdots B_1$	1.698		1.711	1.609	1.668		1.676	1.613
$O_2\cdots H$	2.546		2.375	2.524	2.515		2.621	2.392
$C_2O_1B_1$	128.8		131.4	130.30	129.8		130.8	129.4
$C_2O_1B_1C_1$	−53.1		−61.5	168.10	55.7		58.3	179.2
$C_3C_2O_1B_1$	43.2		−155.0	147.6	−45.1		148.0	−164.8
$O_2C_3C_2O_1$	−120.0		−107.7	−178.34	−85.0		175.8	−106.5
$C_5C_4C_2O_1$	180.0		172.5	−102.45	152.7		−94.1	173.8
$O_1C_2C_4C_5$	72.0		55.3	52.3	66.4		58.0	55.6

[a] For the geometrical parameters considered in this table, see Scheme 5. [b]TS not found.

Scheme 8

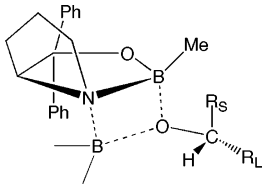

favor S product configuration). Second, reaction C shows that the intrinsic asymmetric induction of the glycosyl derivative **5** leads to major R product formation.

From the previous data one may try to obtain a qualitative prediction of the double asymmetric induction. In other words, one would like to predict the major product configuration resulting from the reaction of the glycosyl derivative **5** with a chiral oxazaborolidine (**1** or **3**). In principle, the answer is simple if one assumes S-type catalysts, since, in that case, both the ketoester and the catalyst favor R product formation (matched pairs).[98] Unsurprisingly, major R product is obtained for reactions E and G.

Prediction of the stereoselectivity for the reduction of **5** with R-type catalysts is less straightforward. Now, the ketoester

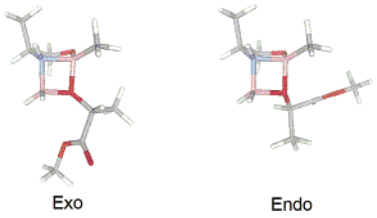

Figure 10. Predicted structure for the oxazadiboroetane intermediate products with R configuration at the newly created chiral center.

Table 15. Oxazadiboretane Intermediate Product Geometry[a] with Calculations for the System with R Configuration at the Newly Created Chiral Center (Values Are in Å and Degrees)

	exo	endo
B_1-N	1.615	1.616
B_2-N	1.586	1.589
B_1-O_1	1.644	1.643
B_2-O_1	1.561	1.563
C_2-O_1	1.428	1.435
C_2-H	1.095	1.094
$HC_2O_1B_1$	51.5	−70.8

[a] For the geometrical parameters considered in this table, see Scheme 4.

Table 16. Summary of Predicted Selectivities for the Reaction Models Considered in This Work

reaction	catalyst	ketoester	main product	de, %
A	**1 (S)**	**4**	R	75.7
B	**3 (S)**	**4**	R	82.8
C	**2**	**5**	R	89.5
D	**1 (R)**	**5**	R	25.1
E	**1 (S)**	**5**	R	94.2
F	**3 (R)**	**5**	S	97.0
G	**3 (S)**	**5**	R	73.2

favors R product, but the catalyst favors S product (mix-matched pairs)[98] and a competition exists. In the case of reaction D that involves the simplest **1(R)** catalyst structure, our calculations suggest that the leading effect is that arising from the chiral ketoester, since major R product is predicted. In contrast, in reaction F, where **3(R)** is used, the asymmetry induced by the glucidic moiety is less pronounced than the oxazaborolidine effect and S product is mainly obtained.

Comparison of the experimental data reported by Coutrot et al.[23] for the galactose derivative in Table 1 with the results in Table 16 for our most realistic model (reactions F−G) indicates a very good agreement. The computations correctly predict the major product configuration as well as the larger value of diastereomeric excess when the R catalyst is used. The comparison of experimental data with the model reactions D−E suggests that **1** is probably too simple a model of the oxazaborolidine catalyst used in the experiments and that such a model seems unsuitable to account for all key interactions.

5. Conclusions

One of the striking results of this work is that glycosyl α-ketoesters do not behave as "normal" ketones when reduced in the presence of oxazaborolidine catalysts. The general picture of this process is that diastereoselectivity is determined by the relative stability of exo/syn and exo/anti transition structures. In Corey's model, exo/syn orientation is favored, and major product configuration is deduced from it. In the case of glycosyl α-ketoesters, such a simple scheme is no longer valid due to

(98) Masamune, S.; Choy, W.; Petersen, J. S.; Sita, L. R.; *Angew. Chem., Int. Ed. Engl.* **1985**, *24*, 1.
(99) Douglas, A. W.; Tschaen, D. M.; Reamer, R. A.; Shi, Y.-J. *Tetrahedron: Asymmetry* **1996**, *7*, 1303.

the low flexibility of the ester group. It may happen that a larger group, such as the galacto-derivative considered in this work, exhibits greater flexibility and plays the role of the "smaller" group. In such a case, the ketone will preferentially coordinate in anti orientation, and the diastereoselectivity will be the opposite of that predicted by means of the standard model. This result is not limited to glycosyl derivatives and might apply to other ketoesters.

When considering a glycosyl α-ketoester, the chirality of the glucidic moiety has to be taken into account. The present study shows that the intrinsic asymmetry induction of the galacto-α-ketoester considered is of the same order of magnitude than that due to a simple chiral oxazaborolidine catalyst. The pyranosyl group asymmetry favors formation of R product. The S-(R-)catalyst favors R(S) product. The final diastereoselectivity is a nonadditive combination of both effects.

Another noticeable result is that the catalyst−borane−ketone complex envisaged in the usual model is predicted to be unstable. It dissociates into a catalyst−borane complex and ketone. This has been pointed out in previous papers dealing with related systems.

Finally, our results show that endo transition structures are possible although they are less stable than the corresponding exo ones. Both endo transition structures (syn and anti) have been located with the simple catalyst **1**, but when methyl groups are placed on the C-5 atom (catalyst **3**), some endo structures are missing. One may expect that, in the CBS catalyst, in which phenyl groups are linked to the C-5 atom, endo structures will become very unfavored or even impossible due to steric repulsion with the large glycosyl α-ketoester molecule. In that case, the diastereofacial selectivity of the catalyst will be basically governed by exo/syn and exo/anti conformations of the transition structures.

Acknowledgment. The authors acknowledge the CNRS computational center CINES (Montpellier, France) for computational facilities (Project lct2550).

Supporting Information Available: Coordinates and energies of all structures, lowest frequencies of vibration (PDF). This material is available free of charge via the Internet at http://pubs.acs.org.

JA031778Y